INTERNATIONAL JOURNAL OF HYDROGEN ENERGY 46 (2021) 15624–15634

Available online at www.sciencedirect.com

ScienceDirect

journal homepage: www.elsevier.com/locate/he

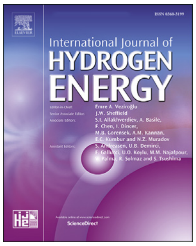

Pressurized hydrogen from charged liquid organic hydrogen carrier systems by electrochemical hydrogen compression

Stephan Mrusek [a], *Patrick Preuster* [b], *Karsten Müller* [b,c],
Andreas Bösmann [a], *Peter Wasserscheid* [a,b,*]

[a] *Lehrstuhl für Chemische Reaktionstechnik, Friedrich-Alexander-Universität Erlangen-Nürnberg, Egerlandstraße 3, D-91058, Erlangen, Germany*
[b] *Forschungszentrum Jülich, "Helmholtz-Institute Erlangen-Nürnberg for Renewable Energies" (IEK 11), Egerlandstraße 3, D-91058, Erlangen, Germany*
[c] *Institute for Technical Thermodynamics, University of Rostock, Albert-Einstein-Straße 2, D-18059, Rostock*

HIGHLIGHTS

- H2 release from LOHC systems is coupled with electrochemical hydrogen compression.
- This combination enhances dehydrogenation rates and provides compressed H2.
- Electrochemical compression produces purified H2 for filling stations.

GRAPHICAL ABSTRACT

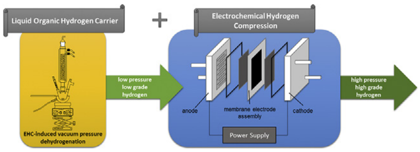

ARTICLE INFO

Article history:
Received 18 December 2020
Received in revised form
2 February 2021
Accepted 3 February 2021
Available online 25 February 2021

Keywords:
Hydrogen storage
Compression
Dehydrogenation
Purity
Heat integration

ABSTRACT

We demonstrate that the combination of hydrogen release from a Liquid Organic Hydrogen Carrier (LOHC) system with electrochemical hydrogen compression (EHC) provides three decisive advantages over the state-of-the-art hydrogen provision from such storage system: a) The EHC device produces reduced hydrogen pressure on its suction side connected to the LOHC dehydrogenation unit, thus shifting the thermodynamic equilibrium towards dehydrogenation and accelerating the hydrogen release; b) the EHC device compresses the hydrogen released from the carrier system thus producing high value compressed hydrogen; c) the EHC process is selective for proton transport and thus the process purifies hydrogen from impurities, such as traces of methane. We demonstrate this combination for the production of compressed hydrogen (absolute pressure of 6 bar) from perhydro dibenzyltoluene at dehydrogenation temperatures down to 240 °C in a quality suitable for fuel cell operation, e.g. in a fuel cell vehicle. The presented technology may be highly attractive for providing compressed hydrogen at future hydrogen filling stations that receive and store hydrogen in a LOHC-bound manner.

---

[*] *Corresponding author.* Lehrstuhl für Chemische Reaktionstechnik, Friedrich-Alexander-Universität Erlangen-Nürnberg, Egerlandstraße 3, D-91058, Erlangen, Germany.

E-mail address: peter.wasserscheid@fau.de (P. Wasserscheid).

https://doi.org/10.1016/j.ijhydene.2021.02.021

Introduction

Liquid organic hydrogen carriers (LOHC) represent a viable and elegant way to safely store and transport hydrogen with high volumetric density using the existing infrastructure for today's hydrocarbon-based fuels. Hydrogen is bound to an organic carrier molecule by catalytic hydrogenation and can be released on demand by catalytic dehydrogenation after an arbitrarily long storage time and/or transporting distance. A carrier system that has attracted particular attention is dibenzyltoluene (H0-DBT)/perhydro dibenzyltoluene (H18-DBT) [1–5]. Due to its high viscosity at low temperatures, adding small amounts of the similar LOHC system benzyltoluene (H0-BT)/perhydro benzyltoluene (H12-BT) with a much lower viscosity might be needed in cold environments [6]. Dibenzyltoluene is known since the 1960s as commercial heat transfer oil for many decades and is cheap (2-6 € depending on quantity and quality) and non-flammable. Moreover, it is excellently suited for storing hydrogen by reversible hydrogenation/dehydrogenation of its three aromatic rings. One molecule of dibenzyltoluene can store up to 9 molecules of hydrogen by hydrogenation enabling a hydrogen loading capacity of 6.2 wt% and a volumetric energy density of 1.9 kWh/L at 20 °C and ambient pressure [7].

The exothermic hydrogenation of H0-DBT is very similar to well-established petrochemical hydrogenation processes and operates with Pt or Ru on alumina catalysts at hydrogen pressures of about 30 bar and temperatures up to 300 °C [3]. Hydrogen mixtures with methane, CO_2 and CO as well as wet hydrogen can be used in the hydrogenation reaction without irreversible catalyst deactivation [3,8]. In contrast, the dehydrogenation is more challenging and less common in the current chemical industry. The reaction is endothermal in character and requires a reaction heat of 65.4 kJ/mol_{H2} (under standard conditions) [9], the same amount of heat that has been released in the exothermal hydrogenation reaction. The nature of the dehydrogenation reaction requires high temperature (e.g. 290 °C–310 °C) and low hydrogen pressure to shift the hydrogenation/dehydrogenation equilibrium towards hydrogen release [4]. At a temperature level of 290 °C and ambient pressure the productivity of a Pt on alumina catalyzed dehydrogenation reaction was found to be between 0.4 and 1.2 $g_{H2}/(g_{Pt}$ min) [4]. The purity of the hydrogen released by the dehydrogenation of H18-DBT can already be up to 99.97 mol% [3], but apart from cyclic hydrocarbons small amounts of methane, CO_2 and CO have to be expected in the hydrogen raw gas if the H18-DBT used is not carefully pre-purified to remove sources of oxygen [10]. The overall LOHC hydrogen storage cycle could be considerably improved if dehydrogenation can proceed at lower dehydrogenation temperature, as this would allow for better heat integration with external heat sources. Of particular interest is a direct heat integration with waste heat generated in the energetic utilization of the released hydrogen, such as waste heat from hydrogen combustion in a hydrogen combustion engine or from a high temperature fuel cell operation [7,11–13].

To enable full dehydrogenation of perhydro dibenzyltoluene at temperatures below 280 °C thermodynamically, the hydrogen partial pressure in the dehydrogenation device can be reduced, thereby shifting the equilibrium to the side of the dehydrogenated species. Fig. 1 shows the pressure/temperature dependence of the reaction equilibrium for the dehydrogenation of the LOHC pair toluene/methylcyclohexane. Similar trends are expected for the chemically very similar system perhydro dibenzyltoluene/dibenzyltoluene.

It can be seen that to achieve technically relevant dehydrogenation conversions of >80% at temperatures <280 °C, the absolute pressure must be below 1 bar. For example, by reducing the pressure to 0.25 bar absolute an equilibrium conversion of 80% is possible at only 230 °C from a thermodynamic point of view. At 0.125 bar absolute 80% hydrogen release is even possible at temperatures as low as 210 °C. The potential of using vacuum pressure to shift the equilibrium conversion to the side of the dehydrogenated species thus enabling low temperature dehydrogenation has already been shown for perhydro benzyltoluene in a reactive distillation column with a temperature of only 200 °C [14].

The reaction rate is positively influenced by the reduction of the absolute pressure as well, as the partial pressure of

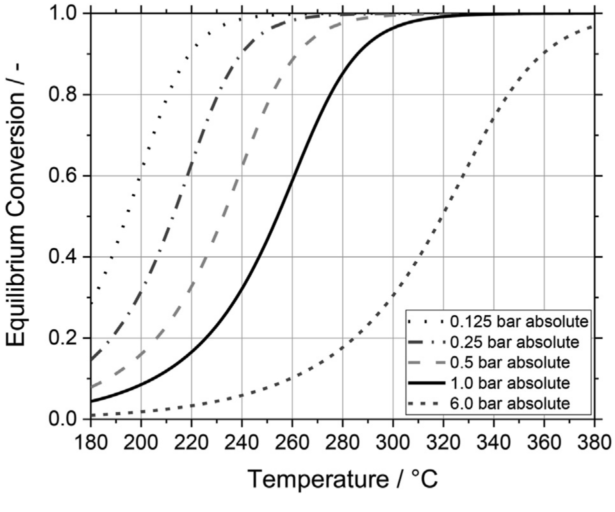

Fig. 1 – Dependence of the equilibrium conversion for the dehydrogenation of methylcylohexane to toluene on temperature and pressure (calculated with AspenPlus V9).

hydrogen is reduced at a given temperature. Assuming a Langmuir-Hinshelwood-Hougen-Watson rate equation for the heterogeneously catalyzed dehydrogenation reaction (Equation (1)) the reduced pressure has a major impact on the driving force of the reaction.

$$r=\frac{(\text{kinetic term}).(\text{driving force or displacement from equilibrium})}{(\text{adsorption term})^{n}} \tag{1}$$

Interestingly, pressure changes in the dehydrogenation reactor provide a very quick way to dynamically change the hydrogen output. The potential for improving the dynamics of the hydrogen release by pressure variation has already been demonstrated by Fikrt et al. [2], but for pressures higher than atmospheric pressure. The ability to dynamically respond to varying hydrogen demand by adjusting the pressure in the dehydrogenation reactor is a strong argument to study in detail the rate and selectivity of catalytic LOHC dehydrogenations under dynamic hydrogen pressure for further advancing the LOHC technology towards practical applications.

A very interesting way to adjust hydrogen pressure in a silent and compact manner using a device that includes no moving parts is electrochemical hydrogen compression (EHC). A schematic diagram is shown in Fig. 2.

In principle, an EHC device is designed as a fuel cell. However, an electrical power source is connected to the two electrodes instead of an electrical load. Hydrogen is conveyed to the anode and oxidized to protons on a carbon-based electrode coated with platinum after passing through a gas diffusion layer (GDL). The electrode is part of a typical membrane electrode assembly (MEA) consisting of a solid polymer electrolyte membrane with electrodes on both sides. The protons produced in this way are forced to selectively pass the membrane while the electrons pass the external electric circuit. The polymer membranes used in EHC devices are often Nafion™ membranes, but polybenzimidazole membranes were gaining some attraction as well [15–17], as they allow higher operation temperatures and consequently offer an enhanced CO-tolerance. Finally, the reduction to elemental hydrogen takes place on the platinum-coated electrode of the cathode side. The voltage needed to operate an EHC device mainly consists of two parts. First, the voltage required for the hydrogen protons to overcome the resistance of the membrane follows Ohm's law. Second, the Nernst voltage allows the transport against a pressure gradient and thus leads to a

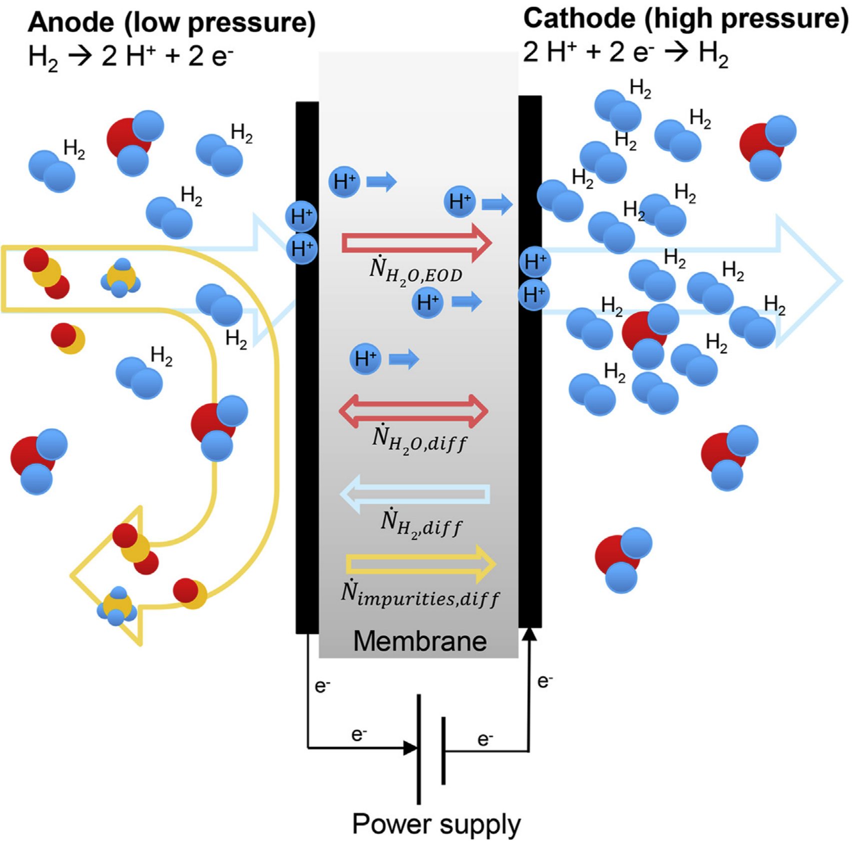

Fig. 2 – Schematic diagram of an electrochemical hydrogen compressor.

compression of hydrogen. The Nernst voltage of the EHC can be calculated by

$$E_{Nernst} = \frac{R \cdot T}{2 \cdot F} \ln\left(\frac{p_{Cathode}}{p_{Anode}}\right) \tag{2}$$

with F the Faraday constant, R the universal gas constant, T the temperature of the cell and $p_{Cathode}$ and p_{Anode} the hydrogen pressures at the cathode and anode side of the EHC device.

Note, however, that at high pressure gradients hydrogen back diffusion from the cathode compartment to the anode compartment can negatively affect the overall efficiency. Another challenge is the water management. Like in fuel cells, the membrane needs to be humidified to provide a proper proton conductivity. There are several mechanisms how water can be transported in the membrane. The two main contributions are diffusion caused by the concentration gradient and the electro-osmotic drag (EOD) where the applied electrical field and the movement of the protons from anode to cathode drag water in the same direction.

Seminal work demonstrating electrochemical hydrogen compression was published by Sedlak et al. already in 1981 [18]. Whereas they predicted 2 MPa as the maximum achievable pressure difference between anode and cathode compartment [18], Grigoriev et al. reported a pressure difference achieved by EHC of 130 bar in 2011 [19]. Since 2012, the Dutch company HyET claims to have realized a hydrogen pressure of 1000 bar in the cathode compartment of their EHC device [20]. Simultaneously to the compression, an implicit purification of the hydrogen takes place, since only protons can cross the membrane with the aid of the applied voltage. Impurities remain almost completely on the anode side as they can only pass the membrane via slow diffusional movements. This type of hydrogen purification by EHC is well described in the literature. Most publications focus on separating hydrogen from inert gases, such as nitrogen [18,21–25], helium [25] or argon [26,27]. Other studies investigate the separation of hydrogen from typical impurities originating from steam methane reforming or partial oxidation in order to produce high quality hydrogen. In these studies the separation of hydrogen from CO and/or CO_2 [15,16,24,28–31], and methane [16,25,26] by the use of EHC has been investigated in detail. As in fuel cells, especially the poisoning of the catalyst with CO is a major challenge in EHC devices. However, several methods to mitigate or avoid catalyst poisoning with CO are feasible including air- and ozone-bleeding [31,32] as well as a self-cleaning due to the electro-oxidation of adsorbed CO at high cell potentials [29,32].

In this contribution we report on a number of highly attractive technological features that arise from the combination of LOHC-bound hydrogen storage, hydrogen release by catalytic dehydrogenation under reduced pressure and hydrogen compression by EHC. In the proposed sequence of unit operations the EHC enables significant process intensification in producing compressed hydrogen from perhydro dibenzyltoluene by simultaneously a) lowering the hydrogen pressure in the anode compartment where the LOHC dehydrogenation takes place thus shifting the reaction equilibrium in favor of low temperature hydrogen release, b) compressing the hydrogen gas in the cathode compartment and c) purifying the released hydrogen by the EHC membrane transport process.

Experimental section

We combined for our studies a typical laboratory setup for the catalytic dehydrogenation of perhydro dibenzyltoluene (H18-DBT) [1,33] with a single-cell electrochemical hydrogen compressor. Fig. 3 shows a simplified flow diagram of our experimental setup.

Reactor part

The dehydrogenation of H18-DBT under reduced pressure induced by the EHC device was carried out in a 100 ml three-neck glass flask heated by a heating mantle and equipped with a condenser. One side neck was closed with a rubber plug and served for temperature measurement (TIC-1) with a thermocouple and for liquid sampling. Argon and hydrogen could be added through the second side neck. The catalyst was added via this side neck with a special loading device. The commercial catalyst applied was platinum supported on alumina in the form of an egg-shell impregnation with 0.3 mass % platinum loading (Clariant, LOT: 101). The H18-DBT (Hydrogenious LOHC Technologies GmbH) was initially placed in the reactor while the catalyst pellets were added to the hot LOHC after the heating up phase. Prior to heating, the reactor was purged via V-1 first with pure argon for inertization and then with hydrogen 5.0 to create a pure hydrogen atmosphere over the reaction mixture and inside the whole setup.

To analyze the progress of the reaction, liquid samples were taken and analyzed using ^{1}H-NMR spectroscopy (Jeol ECX-400). From the NMR spectra the *Degree of Dehydrogenation (DoDH)* was determined according to the method developed by Do et al. [34]. The DoDH describes how much of the hydrogen storable in the LOHC system has been released during dehydrogenation. Based on the DoDHs of two successive liquid samples taken at times t_n and t_{n+1}, it is possible to calculate the productivity P and to assign the latter to the mean DoDH (arithmetic mean) of the specific time interval:

$$P = \frac{(DoDH_{n+1} - DoDH_n) \cdot m_{H2,max}}{m_{Pt} \cdot (t_{n+1} - t_n)} \tag{3}$$

with $m_{H2,max}$ representing the maximum amount of hydrogen storable in the used amount of H18-DBT and m_{Pt} representing the used amount of platinum in the applied catalyst.

The hydrogen produced during the dehydrogenation reaction passed the condenser, in which the LOHC vapors were condensed. However, only a small amount of liquid LOHC droplets was visible in the condenser with hardly no reflux as most of the LOHC stays inside the reactor due to its high boiling point of >370 °C. An activated carbon filter was installed downstream the condenser to remove large organic molecules still present in the hydrogen. The hydrogen reached the anode side of the EHC via the 3-way-valve V-2. The gauge pressure in the system was measured and logged at the inlet of the anode compartment with a stainless steel pressure sensor (PIR-1) type MSD–1/1.5BRE-00-00-GE from GHM Greisinger GmbH.

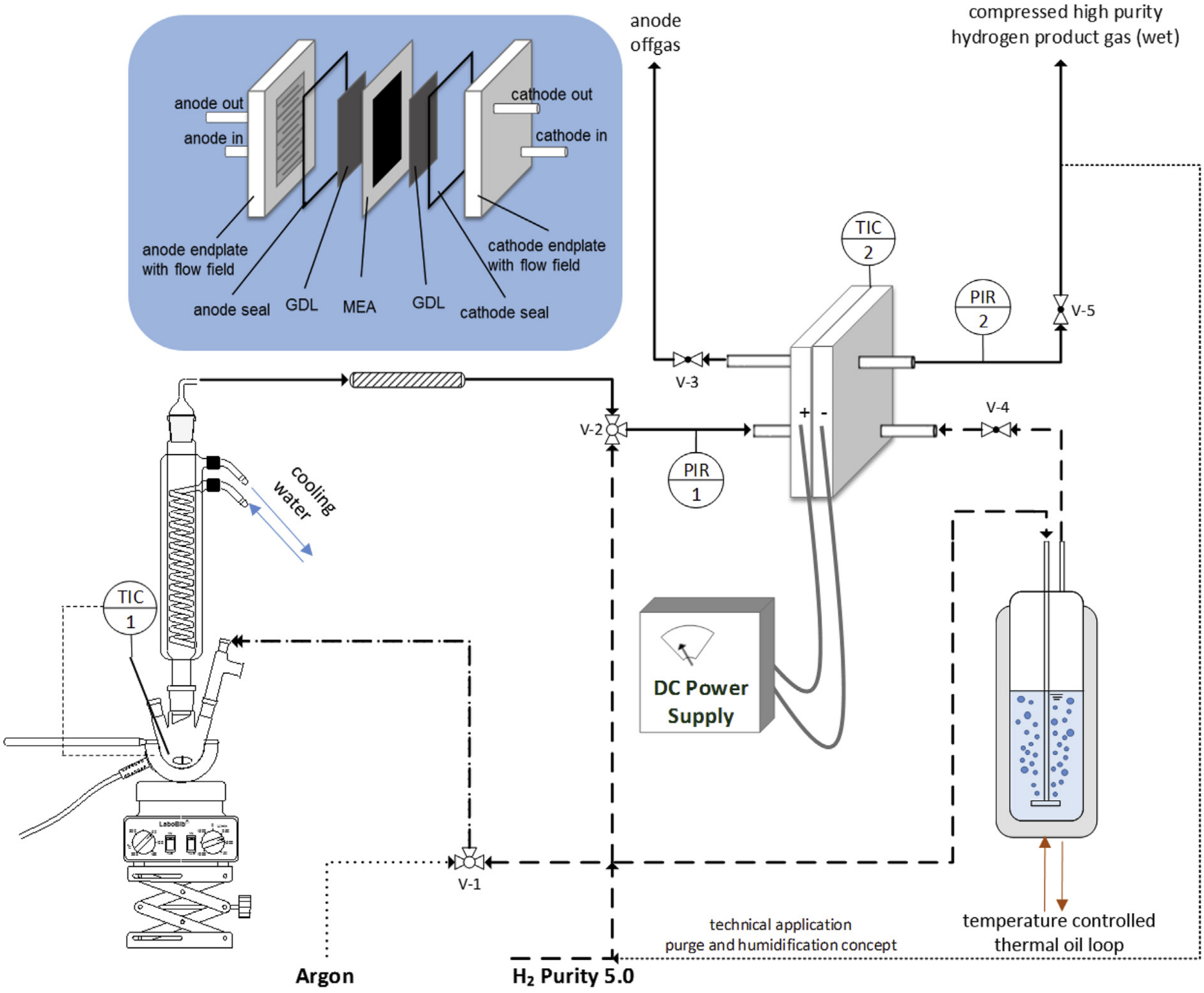

Fig. 3 – LOHC dehydrogenation with hydrogen compression using an EHC device - simplified flow diagram of the setup applied in this study.

EHC part

As an EHC device, a single-cell fuel cell setup from baltic-FuelCells GmbH (qCf FC25/100) with Nafion™ based MEAs from Ion Power was used. The MEAs had an active area of 25 cm^2 and both electrodes had a platinum loading of 0.3 mg/cm^2. The GDLs used on the anode side (Freudenberg H24C3) and at the cathode side (Freudenberg H23C6) had a hydrophobic layer and a microporous layer. The flow fields allowed a meandering hydrogen flow through the anode and cathode compartment. The DC power supply used was from EA-Elektro-Automatik GmbH & Co. KG type EA PS 9040-60 T. The cell could be heated (TIC-2) and cell temperatures between 35 °C and 45 °C were chosen for our experiments.

A special feature of the setup is the humidification of the membrane from the cathode side. Hydrogen 5.0 is passed through a heated humidifier. It is thereby partially saturated with water and provides this water to the cathode side of the membrane in the cell. This type of humidification was required for our purpose because a typical EHC-membrane humidification with the humidifier positioned on the anode side does not work properly under reduced pressure conditions. The reason is that a vacuum pressure corresponding to the vapor pressure of the water in the humidifier would lead to massive water evaporation, and very low partial pressures of hydrogen would reach the anode. In addition, the vapor pressure limits the maximum reachable vacuum pressure. The humidifier in our setup is therefore placed on the cathode side and is heated with thermal oil. The water transported to the EHC device in this way was found to be sufficient to keep the membrane fully hydrated allowing a stable operation. For our conceptual experiments we did not analyze exactly how much water arrived at the cathode and in which state (gaseous or condensed) the water was contacting the electrode material. Interestingly, we found that the state of water at the cathode was obviously less critical as good cell performance and no additional overvoltage was even found in cases where liquid water was present in the cathode compartment. Even with a setup where the membrane was humidified using a liquid water reservoir in the cathode compartment, the cell performance was not negatively affected, a finding that is in good agreement with literature reports [19,35]. We assume that at the stationary operating point of our set-up, the system is fully hydrated and the diffusive water transport from the cathode to the anode of the membrane is in equilibrium with the water transported by EOD from the anode to the cathode.

When the EHC device is connected to the LOHC dehydrogenation reactor to perform hydrogen release experiments under reduced absolute pressure, the anode must be operated in a dead-end mode (ball valve V-3 closed). Accordingly, all hydrogen released by the H18-DBT dehydrogenation must pass through the membrane in the form of protons. Therefore, impurities in the ppm range that reach the anode compartment of the EHC device together with the released hydrogen will accumulate there over time together with air impurities from leakage flows. These impurities lower the hydrogen partial pressure resulting in mass transfer limitations and an increasing cell voltage. Consequently, the anode compartment has to be purged from time to time. This is achieved in our set-up by switching V-2 to pure hydrogen, which causes hydrogen pressure to build up in the anode compartment followed by a brief opening of V-3 to purge the accumulated impurities. In a technical application of the set-up, a small amount of the compressed hydrogen obtained in the EHC device as product gas could be used to realize this occasional purging process.

At the cathode side of the EHC device V-4 and V-5 can be closed to let the hydrogen pressure build up in the cathode compartment. The gauge pressure in this segment can be measured and logged with a stainless steel pressure sensor (PIR-2) type MSD-25BRE-00-00-GE from GHM Greisinger GmbH. During the compression mode of the EHC device, no humidification of the membrane was taking place as the humidifier used in this set-up was made of glass and not able to withstand several bars of hydrogen pressure. Accordingly, the compression was only demonstrated in our setup for a short period of time to prevent the membrane to become dehydrated. The purity of the hydrogen leaving the cathode compartment was analyzed in an FTIR gas analyzer (MultiGas™ 2031 FTIR Continuous Gas Analyzer from mks).

Results and discussion

EHC-induced low pressure dehydrogenation

During a set of initial proof-of-concept experiments it has been found that it is relatively easy to create vacuum pressure with an electrochemical hydrogen compressor during batch dehydrogenation of H18-DBT. Fig. 4 shows two comparative experiments of H18-DBT dehydrogenation at 280 °C for 240 min. The first experiment was carried out without the EHC. Here, the released hydrogen left the dehydrogenation reactor over the entire period of time at ambient pressure. This resulted in a DoDH of 58.2% after 240 min. In the second dehydrogenation experiment, the EHC was switched on after 120 min reaction time. Thus, the conditions in these experiments were identical to the first one for the first 120 min and the DoDHs reached were quite similar. Then, the EHC was set to a current density of 0.2 A/cm^2 and this produced a reduced pressure level in the dehydrogenation reactor. The membrane used in the EHC device was a Nafion™ 117 with a cell temperature of 45 °C. The gauge pressures over time (PIR-1) for this second dehydrogenation experiment with the EHC are presented in Fig. 5.

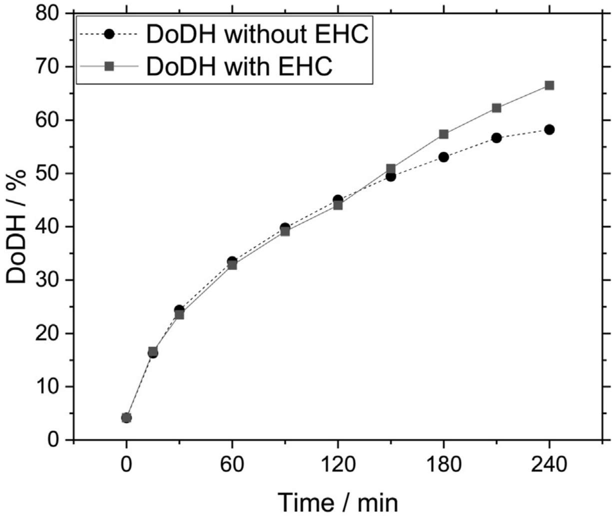

Fig. 4 – Degree of dehydrogenation over time for two dehydrogenation experiments at 280 °C with $n_{H18\text{-}DBT} = 0.05$ mol and $n_{Pt}/n_{H18\text{-}DBT} = 1/2000$. One experiment at ambient hydrogen pressure without EHC and the other with EHC at an applied vacuum pressure of −770 mbar gauge between 120 and 225 min.

After turning the EHC device on, the pressure in the dehydrogenation reactor dropped quickly. After 30 min (150 min total reaction time), a pressure difference to the original ambient conditions of −770 mbar gauge was reached and then maintained for 75 min by manually regulating the current density of the EHC device. During this period the anode side of the EHC device was operated in dead-end mode only interrupted by occasional purging as described above. At 225 min the EHC was switched off and during the last 15 min

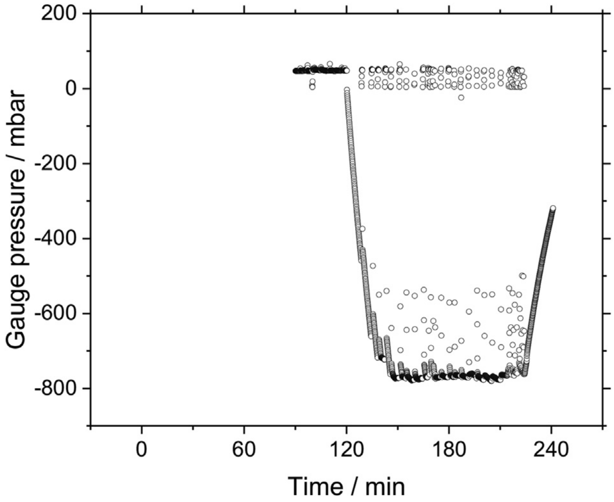

Fig. 5 – Gauge pressure (PIR-1) over time for the dehydrogenation experiment in combination with EHC. The applied vacuum pressure was produced by the EHC starting at 120 min and stopping at 225 min. The scattered points above 0 mbar gauge indicate the occasional purging.

of the experiment the pressure increased due to the released hydrogen of the dehydrogenation reaction. The scattered gauge pressure points in Fig. 5 in between reaction time 120 min and 225 min indicate the purging of the anode with pure hydrogen.

As an important advantage of the present process, the reduced pressure induced by EHC operation led immediately to a significantly improved hydrogen release. After 240 min reaction time, the second experiment (with EHC assistance after 120 min) reached an overall DoDH of 66.5%. During the EHC operation (total reaction times 120–240 min) the ΔDoDH (difference in DoDH at 120 min and 240 min total reaction time) was 22.5% with EHC operation compared to 13.2% without EHC operation reflecting an average increase in the hydrogen release rate of 70% due to the EHC operation. We attribute this significant increase in hydrogen release rate to the increased thermodynamic driving force for dehydrogenation caused by the lower hydrogen partial pressure induced by the EHC operation. Furthermore, a positive influence of the vacuum pressure on the removal of hydrogen from the pore system of the catalyst due to modified conditions for bubble formation, bubble growth and hydrogen transport is assumed to contribute to this enhanced hydrogen release performance.

More details on the EHC voltage and gauge pressure in the dehydrogenation reactor is provided for the time interval of 150–210 min total reaction time (a part of the time interval of reduced pressure operation in our experiment) in Fig. 6.

To keep the dehydrogenation reactor at a constant pressure level of −770 mbar gauge all the hydrogen released from H18-DBT dehydrogenation needs to be transported through the membrane of the EHC device. Due to the batch operation of the reaction and the decreasing reactant concentration the released hydrogen flow decreases over time and the current of the EHC device needs to be adapted accordingly, which was done by manually regulating the power supply. Decreasing the current results in a lower applied voltage.

Fig. 6 illustrates the need for occasional purging on the anode side. In regular time intervals of 3–5 min, a strong voltage increase indicated accumulation of impurities at the anode. These impurities had to be removed by purging to bring the system back to an operation point that remained otherwise very stable over the entire time of EHC operation. Membrane dehydration can be excluded as the reason for the strong voltage increase, as this would not be reversible by simple purging of the anode compartment. No sign of irreversible anode catalyst deactivation was found in our experiment. During the presented time interval of quasi-stable operation (besides the purging events), the required average voltage for maintaining the vacuum pressure by pumping the released hydrogen through the membrane was in our device 0.1233 V. This corresponds to a specific energy need of 3.3 kWh/kg_{H2} or the equivalent of 10% of the lower heating value (LHV) of the pumped hydrogen. The average current between 150 and 210 min total reaction time was 2.62 A and the average current density was approx. 0.1 A/cm^2. This corresponds to a hydrogen pumping capacity of 18.24 Nml/min through the 25 cm^2 active membrane area. As expected from mass balance consideration, a very similar value of $V_{H2} = 19.08$ Nml/min is found by calculating the average hydrogen release rate during dehydrogenation, which can be determined from the difference in DoDH between 150 and 210 min total reaction time. This proves that the EHC pumps all the released hydrogen under the applied reaction and operation conditions.

A further dehydrogenation experiment with EHC-induced pressure reduction was carried out at a reactor temperature of 260 °C. The pressure reduction caused by the EHC device was −500 mbar gauge in this case while the cathode side remained at ambient pressure. This time, the reduced pressure was already produced in the reactor by EHC operation before the catalyst was added to the heated H18-DBT and it was maintained over the entire 240 min of the experiment. Fig. 7 and Fig. 8 illustrate the DoDH as a function of reaction

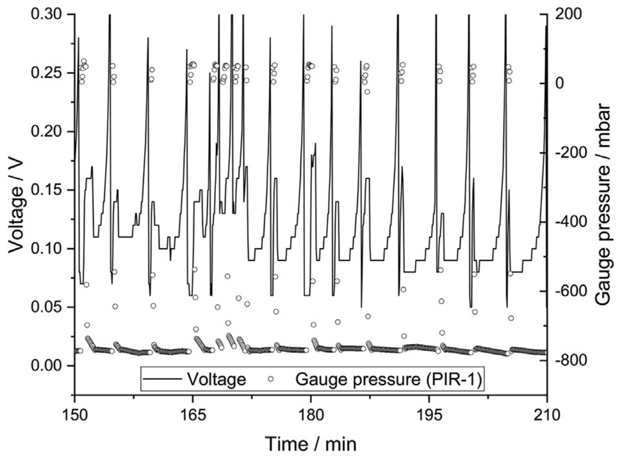

Fig. 6 – Applied voltage for the EHC and gauge pressure (secondary axis) achieved by EHC operation over time between 150 – 210 min of our H18-DBT dehydrogenation experiment; other results shown in Figs. 4 and 5.

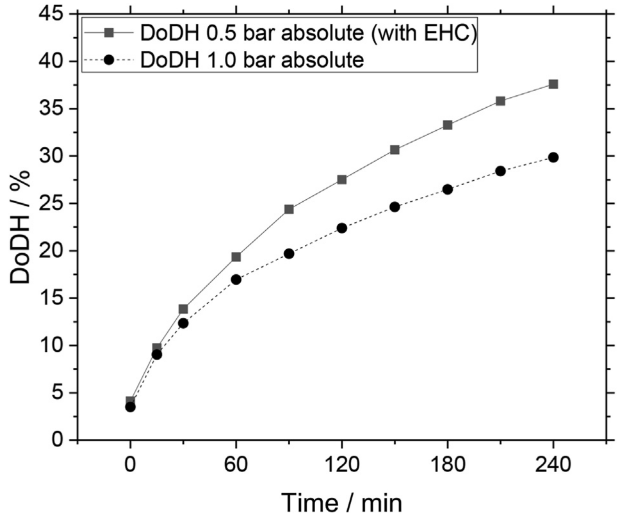

Fig. 7 – DoDH over time for two dehydrogenation experiments at 260 °C with $n_{H18\text{-}DBT} = 0.05$ mol and $n_{Pt}/n_{H18\text{-}DBT} = 1/2000$: One experiment at ambient hydrogen pressure (1.0 bar absolute) without EHC assistance and one experiment with an EHC-induced reduced pressure of 0.5 bar absolute.

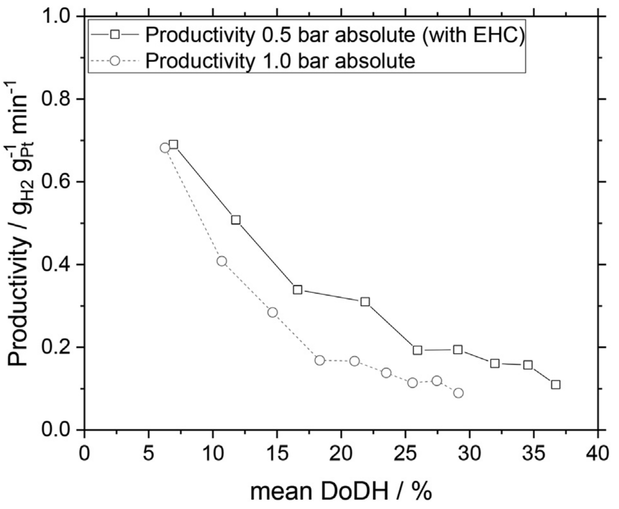

Fig. 8 – Productivity over DoDH for two dehydrogenation experiments at 260 °C with $n_{H18\text{-}DBT} = 0.05$ mol and $n_{Pt}/n_{H18\text{-}DBT} = 1/2000$: One experiment at ambient hydrogen pressure (1.0 bar absolute) without EHC assistance and one experiment with an EHC-induced reduced pressure of 0.5 bar absolute.

time and the dehydrogenation productivity over the mean DoDH. Again, we compare two experiments, one without EHC operation with hydrogen release at ambient pressure (1.0 bara) and one with EHC-promoted operation at a pressure of 0.5 bar absolute.

Again, the dehydrogenation rate is significantly increased by the EHC-induced pressure reduction in the dehydrogenation reactor. With progress in conversion a clear difference in dehydrogenation rate between the two experiments is found. As comparison of rates should take place at similar DoDH (or H18-DBT conversion), we selected three distinct points for comparison with almost identical DoDH in both experiments (deviation less than 1%, see Table 1). It was found that the productivity at the same mean DoDH was between 1.69 and 2.17 times higher in the EHC-induced reduced pressure experiment. Having a look at the calculated equilibrium conversion of MCH/toluene dehydrogenation/hydrogenation in Fig. 1 and assuming the equilibrium of H18-DBT/H0-DBT showing the same trends, one can see that at a temperature of 260 °C and an absolute pressure of 0.5 bar the equilibrium conversion is approximately 88% compared to approximately 59% at 1 bar absolute. Using these values, the distance from the equilibrium conversion can be calculated at the three distinct points for comparison in Table 1. It is then found that the ratios of the distances to the equilibrium conversion are similar to productivity ratios pointing out that the increased hydrogen release rate correlates to the increased distance from the reaction equilibrium. This demonstrates impressively the effect of pressure reduction for the low temperature hydrogen release from pure hydrocarbon LOHC systems.

Electrochemical hydrogen compression of hydrogen released from H18-DBT

In the experiments described so far, ambient hydrogen pressure was produced at the cathode side of the applied EHC unit. Still, electrochemical hydrogen compression took place, but only from vacuum pressure on the anode side to ambient pressure at the cathode side. Electrochemical hydrogen compression from 0.5 bar absolute to ambient pressure corresponds, for example, to a compression factor of 2 and, at a temperature of 45 °C, to a Nernst voltage of 9.5 mV (see Equation (2)). In order to prove that compressed hydrogen can be produced from H18-DBT by the help of the applied EHC device, the valves V-4 and V-5 on the cathode side of the EHC were closed during an EHC-supported dehydrogenation experiment at 260 °C and a pressure in the anode chamber of 0.5 bar absolute. Doing so, pressure was built up in the cathode chamber between V-4 and V-5. Since the two half-cells of the EHC unit were held together pneumatically with compressed air, the maximum hydrogen pressure in our EHC device was limited to a pressures of 6 bar absolute. In this experiment the weighed masses of LOHC and catalyst were 29 g and 3.25 g, respectively, resulting in a catalyst to LOHC ratio $n_{Pt}/n_{H18\text{-}DBT}$ of 1:2000. The membrane used was a Nafion™ 1110 with a cell temperature of 45 °C. No humidification of the membrane could take place during the pressure build-up. Due to the dead-end operation of the EHC device on both sides (anode and cathode outlets were both closed for pressure build-up), however, no water was lost and a stable operation of the EHC was possible. Before starting the compression and shortly before reaching the maximum pressure of 6 bar absolute, the anode was purged with pure hydrogen in order to evaluate the overlaying excess voltage due to impurities accumulating at the anode side of the EHC unit (see above). The gauge pressures on the anode (PIR-1) and cathode side (PIR-2) are shown in Fig. 9 for a compression to 6 bar absolute with the EHC at a current density of 0.1 A/cm^2. The linear increase in the cathode pressure over time is clearly visible indicating a negligible dependence of the back diffusion on the pressure difference and a non-existent leakage in the pressure range considered. Note, that the combined action of H18-DBT dehydrogenation at 260 °C/0.5 bar absolute and EHC compression delivers

Table 1 – Comparison of productivities and of the distances from reaction equilibrium of two H18-DBT dehydrogenation experiments at 1 bar absolute and 0.5 bar absolute (EHC-induced) at three distinct points of very similar DoDH that where reached after different reaction times; reaction conditions: 260 °C, $n_{H18\text{-}DBT} = 0.05$ mol, $n_{Pt}/n_{H18\text{-}DBT} = 1/2000$.

mean DoDH/%		productivity/$g_{H2}g_{Pt}^{-1}min^{-1}$		distance from equilibrium/%		productivity ratio	distance from equilibrium ratio
1.0 bar	0.5 bar	1.0 bar	0.5 bar	1.0 bar	0.5 bar		
21.04	21.87	0.17	0.31	38	67	1.86	1.76
25.56	25.95	0.11	0.19	33	63	1.69	1.9
29.14	29.09	0.09	0.19	30	60	2.17	2.00

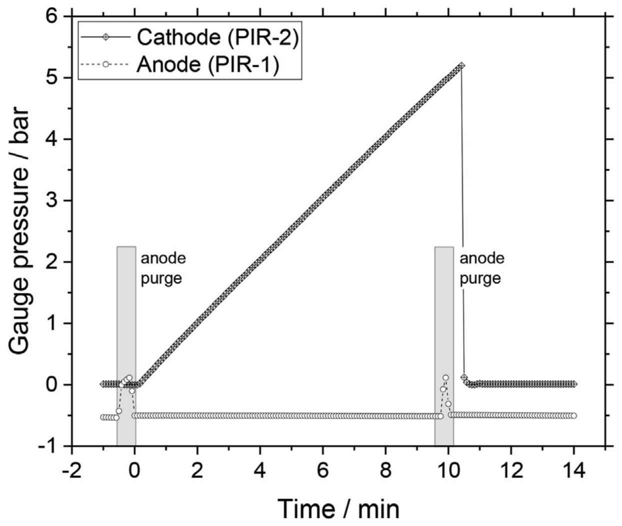

Fig. 9 – Gauge pressures at anode and cathode during compression experiments with the EHC. A dehydrogenation experiment with −0.5 bar gauge EHC-induced vacuum pressure and 260 °C is connected to the anode side of the EHC.

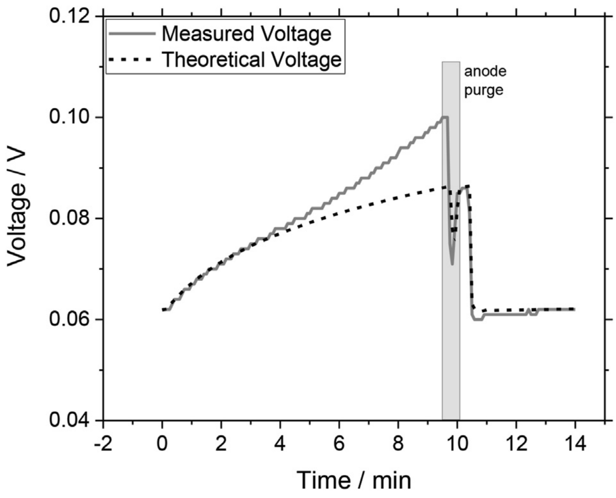

Fig. 10 – Measured and theoretical voltage during the compression to 6 bar absolute at the cathode side of the EHC. The theoretical voltage is calculated based on Equation (2) and a value of 52.5 mV is added as the voltage to overcome the membrane resistance.

hydrogen at 6 bar absolute. To reach the same pressure with the same level of reachable degree of dehydrogenation (90% DoDH) by a thermal dehydrogenation process alone would require a temperature of about 360 °C for thermodynamic reasons (see Fig. 1). Such elevated temperature is at the thermal stability limit of H0-DBT, and thus operation at these conditions would lead to some decomposition of the applied hydrogen carrier.

The cell voltage required during the compression was measured with a Voltcraft BB-500 handheld multimeter directly at the cell and is not, as in the earlier results presented, the value displayed by the power supply. Note, that the measured cell voltage is always a few mV lower than the applied voltage of the DC power supply, as there are no conduction losses.

The measured cell voltage during the compression experiment is shown in Fig. 10. At the beginning of compression and directly after an initial purge of the anode compartment, a cell voltage of 62 mV was found to transport the hydrogen provided via dehydrogenation through the membrane. This voltage already includes the Nernst voltage for the compression from 0.5 bar absolute on the anode side to ambient pressure on the cathode side ($E_{Nernst} = 9.5$ mV). Thus, a voltage of 52.5 mV was found necessary to overcome the cell resistance. Fig. 10 shows – next to the measured values – the theoretical Nernst voltage based on Equation (2) ($T_{cell} = 45$ °C). The value of 52.5 mV has been added to the calculated Nernst voltage to make the calculated and the measured graphs comparable. It can be seen that at the beginning of the compression, the increase in cell voltage followed the course of the theoretical Nernst voltage and an isothermal electrochemical hydrogen compression took place. After 4 min compression time, the measured value started to deviate from the theoretical value. However, by purging the anode shortly before the maximum pressure was reached at the cathode side, the measured cell voltage could be brought back to the value of the theoretical voltage. Therefore, the additional cell voltage is most likely the result of gaseous components other than hydrogen accumulating in the anode compartment and leading to mass transport limitations and the increased cell voltage. Accordingly, hydrogen compression at the cathode side is expected to be isothermal, which is also indicated by the fact that the cell voltage drops from 86 mV to 61 mV by releasing the cathode pressure back to ambient. This difference corresponds almost exactly to the Nernst voltage for compression from ambient pressure to 6 bara of 24.6 mV.

Comparing in an idealized calculation the energy needed for the electrochemical compression from 0.5 bar absolute to 6 bar absolute with the additional thermal energy requirement to increase the temperature in the dehydrogenation from 260 °C to 360 °C (to realize a similar hydrogen pressure by the thermal dehydrogenation thermodynamically) one obtains values in a comparable range. With the compression factor of 12 a Nernst voltage of 34.1 mV can be calculated which equals to a specific energy requirement of 0.91 kWh/kg_{H2} to deliver hydrogen at 6 bar absolute. In comparison, only the additional heating of fully loaded H18-DBT by another 100 °C results in an additional specific energy requirement of approximately 0.71 kWh/kg_{H2} [9]. Note, however, that it is easier to find heat sources at lower temperatures and that at 360 °C the decomposition of H18-DBT leads to additional restrictions and challenges.

With a differently designed EHC unit it should be possible to reach higher pressures at the cathode side. A theoretical estimation for providing hydrogen at a pressure level of 50 bar absolute (the pressure level of the mass storage of a typical hydrogen filling station) on the cathode and 0.5 bar absolute on the anode side (to drive H18-DBT dehydrogenation, resulting in a compression factor of 100) indicates a required Nernst voltage of 63 mV, which corresponds to a specific energy consumption of 1.69 kWh/kg_{H2}.

Table 2 – Impurity levels in ppm in (i) the H_2 released by dehydrogenation from perhydro dibenzyltoluene (raw gas); (ii) the H_2 at the outlet of the EHC, i.e. a mixture of EHC-purified H_2 from the dehydrogenation mixed with humidified H_2 (quality 5.0), and (iii) H_2 (quality 5.0) used for humidification of the membrane of the EHC.

	methane	CO	CO_2	hydrocarbons ($\geq C_2$)[a]
(i) H_2 from dehydrogenation without EHC (raw gas)	120.47	1.49	6.90	93.81
(ii) EHC purified H_2 mixed with humidified H_2 (quality 5.0) at an average mixture ratio of 0.625	0.09	0.00	0.00	1.94
(iii) H_2 (quality 5.0, house gas)	0.04	0.00	0.01	1.98

[a] The $\geq C_2$ hydrocarbons detected consist mainly of ethane and C_6 to C_7 cyclics, such as toluene, methylcyclohexane, benzene and cyclohexane.

EHC-based hydrogen purification

In order to examine the purification effect of the applied EHC device on the hydrogen released from perhydro dibenzyltoluene, a dehydrogenation experiment at 240 °C at 0.5 bar absolute with EHC assistance was performed and compared with an experiment without EHC at 240 °C at 1.0 bar absolute. The experiments were carried out using a catalyst to LOHC ratio of $n_{Pt}/n_{H18\text{-}DBT}$ of 1/1000 ($m_{H18\text{-}DBT} = 29$ g and $m_{cat,\ total} = 6.25$ g). The activated carbon filter was bypassed in this case to observe the performance of the EHC device in the presence of all impurities present in the raw hydrogen from LOHC dehydrogenation. A Nafion™ 115 membrane was used in this set of experiments with a cell temperature of 35 °C. The purity of the hydrogen was analyzed with the FTIR gas analyzer. The impurity levels were averaged over a reaction time of 3 h and are displayed in Table 2.

It should be noted that the hydrogen at the outlet of the cathode compartment analyzed in the case of the EHC-induced purification is a mixture of the hydrogen released by dehydrogenation with downstream EHC purification and the humidified house gas hydrogen (quality 5.0) applied for humidifying the EHC at the cathode side. Therefore, we give the purity of the applied house gas hydrogen (quality 5.0) used for membrane humidification as well in Table 2. The latter was determined by switching off the EHC after the end of the experiment and analyzing the pure house gas hydrogen only (averaged over 1.5 h).

The volume flow of the house gas hydrogen for humidifying the membrane of the EHC device on the cathode side was 40 Nml/min. Due to the dehydrogenation in batch mode, the flow of released hydrogen decreased with increasing reaction time and can be determined via the electric current of the EHC (see above). The electric current for maintaining the vacuum in the dehydrogenation experiment with EHC varied between values of 10 A (0.4 A/cm^2) at the beginning of the experiment and 1.8 A (0.07 A/cm^2) after 3 h of the experiment, which corresponds to volume flows of the released hydrogen of 70 Nml/min and 12.5 Nml/min respectively. From these values, the ratio of purified hydrogen from dehydrogenation to added hydrogen for humidification can be calculated. This ratio was 1.75 at the beginning of the experiment and 0.31 after 3 h reaction time. Averaged over time, a current of 3.65 A was applied, resulting in an average ratio of 0.625.

A comparison of the impurity level of the raw gas from the dehydrogenation with the purities of the hydrogen purified by EHC impressively demonstrates the cleaning performance of the EHC. All impurities could be removed to a considerable extent. Instead of the 120 ppm, only 0.09 ppm methane was found and CO and CO_2 could not be detected at all. Higher hydrocarbons were also retained by the EHC process. The level of around 2 ppm is identical to that found in the hydrogen 5.0 house gas. Summing up, the combined level of all impurities was 223 ppm in the hydrogen raw gas released by dehydrogenation from H18-DBT and only 2 ppm in the EHC-purified (and diluted) hydrogen derived from H18-DBT under the applied conditions.

Conclusion

In this contribution we demonstrate that the combination of hydrogen release from the hydrogen-charged, pure hydrocarbon LOHC compound H18-DBT and electrochemical hydrogen compression provides three very attractive and technically relevant features: a) The rate of dehydrogenation is increased between 69 and 117% by the increased driving force for dehydrogenation caused by the EHC-induced pressure reduction under otherwise identical reaction conditions; b) The hydrogen is compressed by the EHC operation. We have demonstrated in our set-up a compression factor of 12 that was only limited by the construction of the applied EHC device; c) The hydrogen formed at the cathode from the pumped protons has shown to be extremely pure. According to our investigations, the total level of impurities is only 2 ppm on a dry basis and the hydrogen is free of any fuel cell poisons.

We achieved this combination of EHC-induced, reduced pressure LOHC dehydrogenation and EHC-induced, hydrogen compression in a quite simple experimental setup. Occasional purging of the anode compartment was found necessary to prevent mass transport limitations due to the accumulation of gaseous impurities. With the purging, the anode catalyst showed no irreversible degradation over at least 4 h. The specific energy consumption of the EHC operation was found to be quite small in comparison to the energy required typically for mechanical hydrogen compression. According to the commercial producers of EHC units [20], much higher hydrogen pressures can be reached with commercially available EHC devices, certainly up to the pressure level of 50 bar absolute that is required for the hydrogen mass storage of typical hydrogen filling stations.

It can thus be concluded that the EHC operation provides a great potential for producing high quality, pressurized hydrogen from LOHC-bound hydrogen by reducing the dehydrogenation temperature, by compressing and cleaning hydrogen at the same time using a single device. The energetic advantage of the here-proposed “hydrogen-charged LOHC to compressed hydrogen” process increases drastically, if the reduced temperature level enabled by the reduced pressure opens otherwise untouchable potentials for waste heat integration.

For the specific application case of hydrogen delivery to future hydrogen filling stations, the LOHC dehydrogenation/EHC combination can offer wet but otherwise very pure hydrogen at the required pressure level of the hydrogen mass storage. Moreover, this combination guaranties intrinsically fuel cell-proven hydrogen quality by the successful operation of the EHC's anode catalyst. Thus, the here described technology has the potential to greatly contribute to improved energy efficiency, cost, reliability and resilience of future hydrogen filling station utilizing hydrogen supplied and stored in LOHC-bound form.

Declaration of competing interest

The authors declare the following financial interests/personal relationships which may be considered as potential competing interests: Peter Wasserscheid is founder and minority share holder of the company Hydrogenious LOHC technologies (www.hydrogenious.net) that offers commercially hydrogen storage systems based on the LOHC technology.

There is no conflict of interest to declare with regard to the specific scientific results reported in this paper.

Acknowledgement

The authors like to thank Gabriel Sievi and Alexander Bulgarin for fruitful discussions. They gratefully acknowledge infrastructural support by the Bavarian Ministry of Economic Affairs, Regional Development and Energy, and by the BMBF through the cluster B1 of the Kopernikus “Power2X” project. This project has received funding from the Fuel Cells and Hydrogen 2 Joint Undertaking under the European Union's Horizon 2020 research and innovation programme under grant agreement No. 779694.

REFERENCES

[1] Brückner N, Obesser K, Bösmann A, Teichmann D, Arlt W, Dungs J, Wasserscheid P. ChemSusChem 2014;7:229–35.
[2] Fikrt A, Brehmer R, Milella V-O, Müller K, Bösmann A, Preuster P, Alt N, Wasserscheid P, Arlt W. Appl Energy 2017;194:1–8.
[3] Jorschick H, Vogl M, Preuster P, Bösmann A, Wasserscheid P. Int J Hydrogen Energy 2019;44(59):31172–82.
[4] Jorschick H, Preuster P, Dürr S, Seidel A, Müller K, Bösmann A, Wasserscheid P. Energy Environ Sci 2017;10(7):1652–9.
[5] Modisha PM, Jordaan JHL, Bösmann A, Wasserscheid P, Bessarabov D. Int J Hydrogen Energy 2018;43(11):5620–36.
[6] Jorschick H, Geißelbrecht M, Eßl M, Preuster P, Bösmann A, Wasserscheid P. Int J Hydrogen Energy 2020;45(29):14897–906.
[7] Preuster P, Papp C, Wasserscheid P. Acc Chem Res 2017;50(1):74–85.
[8] Jorschick H, Bulgarin A, Alletsee L, Preuster P, Bösmann A, Wasserscheid P. ACS Sustainable Chem Eng 2019;7(4):4186–94.
[9] Müller K, Stark K, Emel Yanenko VN, Varfolomeev MA, Zaitsau DH, Shoifet E, Schick C, Verevkin SP, Arlt W. Ind Eng Chem Res 2015;54(32):7967–76.
[10] Bulgarin A, Jorschick H, Preuster P, Bösmann A, Wasserscheid P. Int J Hydrogen Energy 2020;45(1):712–20.
[11] Müller K, Thiele S, Wasserscheid P. Energy Fuels 2019;33(10):10324–30.
[12] Preuster P, Fang Q, Peters R, Deja R, Blum L, Stolten D, Wasserscheid P. Int J Hydrogen Energy 2018;43(3):1758–68.
[13] Peters R, Deja R, Fang Q, Preuster P, Blum L, Wasserscheid P, Stolten D. Int J Hydrogen Energy 2019;44(26):13794–806.
[14] Geißelbrecht M, Mrusek S, Müller K, Preuster P, Bösmann A, Wasserscheid P. Energy Environ Sci 2020;13(9):3119–28.
[15] Perry KA, Eisman GA, Benicewicz BC. J Power Sources 2008;177(2):478–84.
[16] Thomassen M, Sheridan E, Kvello J. J Nat Gas Sci Eng 2010;2(5):229–34.
[17] Kim SJ, Lee B-S, Ahn SH, Han JY, Park HY, Kim SH, Yoo SJ, Kim H-J, Cho E, Henkensmeier D, Nam SW, Lim T-H, Kim S-K, Huh W, Jang JH. Int J Hydrogen Energy 2013;38(34):14816–23.
[18] Sedlak JM, Austin JF, LaConti AB. Int J Hydrogen Energy 1981;6(1):45–51.
[19] Grigoriev SA, Shtatniy IG, Millet P, Porembsky VI, Fateev VN. Int J Hydrogen Energy 2011;36(6):4148–55.
[20] Bouwman P. Fundamentals of electrochemical hydrogen compression. In: Bessarabov D, Wang H, Li H, Zhao N, editors. PEM electrolysis for hydrogen production – principles and applications. Taylor & Francis Group LLC; 2016. p. 269–302.
[21] Lee HK, Choi HY, Choi KH, Park JH, Lee TH. J Power Sources 2004;132(1–2):92–8.
[22] Onda K, Ichihara K, Nagahama M, Minamoto Y, Araki T. J Power Sources 2007;164(1):1–8.
[23] Casati C, Longhi P, Zanderighi L, Bianchi F. J Power Sources 2008;180(1):103–13.
[24] Onda K, Araki T, Ichihara K, Nagahama M. J Power Sources 2009;188(1):1–7.
[25] Nordio M, Rizzi F, Manzolini G, Mulder M, Raymakers L, Annaland MVS, Gallucci F. Chem Eng J 2019;369:432–42.
[26] Ibeh B, Gardner C, Ternan M. Int J Hydrogen Energy 2007;32(7):908–14.
[27] Doucet R, Gardner CL, Ternan M. Int J Hydrogen Energy 2009;34(2):998–1007.
[28] Farooque M, Kush A, Abens S. Separ Sci Technol 1990;25(13–15):1361–73.
[29] Gardner CL, Ternan M. J Power Sources 2007;171(2):835–41.
[30] Abdulla A, Laney K, Padilla M, Sundaresan S, Benziger J. AIChE J 2011;57(7):1767–79.
[31] Nordio M, Barain ME, Raymakers L, Annaland MVS, Mulder M, Gallucci F. Chem Eng J 2020;392:123647.
[32] Jackson C, Raymakers LFJM, Mulder MJJ, Kucernak ARJ. J Power Sources 2020;472:228476.
[33] Auer F, Blaumeiser D, Bauer T, Bösmann A, Szesni N, Libuda J, Wasserscheid P. Catal Sci Technol 2019;9(13):3537–47.
[34] Do G, Preuster P, Aslam R, Bösmann A, Müller K, Arlt W, Wasserscheid P. React Chem Eng 2016;1(3):313–20.
[35] Hao Y, Nakajima H, Yoshizumi H, Inada A, Sasaki K, Ito K. Int J Hydrogen Energy 2016;41(32):13879–87.